*Molecular Simulation*, Vol. 31, No. 5, April 2005, 339–347

Taylor & Francis
Taylor & Francis Group

# A computational study of the effect of Li–K solid solutions on the structures and stabilities of layered silicate materials—an application of the use of Condor pools in molecular simulation

Z. DU†, N. H. DE LEEUW†,‡*, R. GRAU-CRESPO†, P. B. WILSON§, J. P. BRODHOLT§, M. CALLEJA¶ and M. T. DOVE¶

†School of Crystallography, Birkbeck College, University of London, Malet Street, London WC1E 7HX, UK
‡Department of Chemistry, University College London, 20 Gordon Street, London WC1H 0AJ, UK
§Department of Earth Sciences, University College London, Gower Street, London WC1E 6BT, UK
¶Department of Earth Sciences, University of Cambridge, Downing Street, Cambridge CB2 3EQ, UK

*(Received July 2004; in final form September 2004)*

Computer modelling techniques were used to investigate the structures and stabilities of Li–K solid solutions of three different disilicate structures, employing a newly developed program based on symmetry arguments to identify identical configurations and hence eliminate unnecessary duplication of calculations. Even so, the large number of calculations needed to sample the complete set of configurations of a wide range of solid solutions necessitated the use of an extensive Condor pool of PC clusters, which afforded the necessary computing resources for this study.

The results of our calculations show that in the wide range of Li–K solid solutions investigated, the mixed-cationic $KLiSi_2O_5$ material retains its original structure when the composition was varied, where six-membered rings of silica tetrahedra are linked to form continuous channels throughout the structure. The channel positions are found to be preferentially occupied by the potassium ions rather than by the smaller lithium ions. The original framework of the experimental $K_2Si_2O_5$ structure, containing 14-membered rings of silica tetrahedra, similarly remains intact with the introduction of smaller lithium atoms into the bigger potassium lattice sites. However, the replacement of potassium ions for lithium ions in the $Li_2Si_2O_5$ material causes significant distortions of the original structure, which loses its symmetry, although the ring structure remains.

*Keywords*: Layered silicates; Phyllosilicate; Solid solutions; Cation ordering

## 1. Introduction

Silicates are multi-functional materials and due to their importance in electronic, optical and biomedical applications, as well as their dominance in geological environments, they have particular appeal to a variety of scientific communities. Over the last years, mixed alkali-disilicates ($M_2Si_2O_5$) have attracted attention due to their anomalous behaviour, leading to extensive experimental and computational investigations which are summarised by Day [1], Ingram [2] and Isard [3]. For example, some alkali disilicates are very sensitive to moisture, whereas others are not, and the mutual interactions of more than one alkali metal in the material may play a significant role in their distinctive hydration properties. Other studies indicate that transport properties in mixed alkali disilicates depend on their composition in a non-linear way [1,2], which is known as the mixed alkali effect. Habasaki and co-workers [4] carried out molecular dynamics simulations to determine the mixed alkali effect and they concluded that mobility of the cations was reduced in a mixed alkali material, due to a site memory effect leading to a lower probability of a cation moving to a site previously occupied by the other type of cation. Matsumoto and co-workers [5] have also used molecular dynamic simulations to study structures and energetic properties of mixed alkali silicates, which showed that introduction of the larger alkali component into the structure led to a shorter bond length between the alkali ions and the oxygen ions and vice versa for the smaller alkali metal ion.

However, so far all previous studies were based on materials of either single-alkali disilicates or mixed-alkali disilicates with equal amounts of the two metal components. No systematic investigation across the whole range of solid solutions has been reported, even though it is of fundamental interest to study the effect of the change in composition of

*Corresponding author. School of Crystallography, Birkbeck College, University of London, Malet Street, London WC1E 7HX, UK.
E-mail: n.deleeuw@mail.cryst.bbk.ac.uk

*Molecular Simulation*
ISSN 0892-7022 print/ISSN 1029-0435 online © 2005 Taylor & Francis Group Ltd
http://www.tandf.co.uk/journals
DOI: 10.1080/08927020500067013

the mixed-alkali disilicates and the cation distribution on the structures and stabilities of these materials. In this work, we have employed interatomic potential-based simulations, using static lattice energy calculations, to investigate the effect of cation distribution on the structures and stabilities of a series of Li–K solid solutions of three different disilicate materials.

In addition to the intrinsic scientific interest, the need to calculate many hundreds of different configurations for each composition, for which we have used a Condor pool of PC clusters [6], makes this work a good example of the application of Condor pools to combinatorial computational chemistry.

## 2. Methodology

The structures and energies of the Li–K solid solutions of the different disilicate materials were modelled using classical energy minimisation techniques. These atomistic simulation methods are based on the Born model of solids [7], which assumes that the ions in the crystal interact *via* long-range electrostatic forces and short-range forces, including both the repulsions and the van der Waals attractions between neighbouring electron charge clouds, which are described by simple analytical functions. The electronic polarisability of the ions is included *via* the shell model of Dick and Overhauser [8] in which each polarisable ion, in our case the oxygen ion, is represented by a core and a massless shell, connected by a spring. The polarisability of the model ion is then determined by the spring constant and the charges of the core and shell. When necessary, angle-dependent forces are included to allow directionality of bonding as, for example, in the O—Si—O interactions.

The lattice energies of the pure and mixed structures were calculated using the energy minimisation code METADISE [9], where periodic boundary conditions and sufficiently large supercells are employed to avoid surface and finite size effects and interactions between the repeating images. For each Li–K composition, all possible configurations are calculated, leading to a large number of different final structures, all with different lattice energies. Although the energies of some of these final structures for each composition lie within a few kilojoules of each other and hence could be expected to occur experimentally to some extent, we found that configurations with similar energies usually had similar lattice structures. As such only the configuration with the lowest lattice energy for each Li–K composition is selected to represent the final structure for discussion in this work.

### 2.1 Interatomic potential model

We have employed established potential parameters from previous studies for the simulations of these layered silicate structures. The potential model by Sanders *et al.* [10] is used for the simulation of the silicate framework, which has been used for a wide selection of silicate materials, ranging from semi-covalent quartz [11] and open framework structures [12] to more ionic materials such as $Mg_2SiO_4$, where the silicate group acts as a polyanion [13]. This potential model assigns integral ionic charges of $+4$ and $-2$ to the silicon and oxygen atoms, respectively and as already mentioned above, it also includes a three-body O—Si—O bond-bending term to account for directionality in the partially covalent Si—O bond, in addition to short-range Buckingham potentials to describe the Si—O and O—O interactions [10].

The interactions between the alkali ions and the oxygen atoms are described by the potential parameters from the work of Purton and co-workers [14] in their work on solution energies of heterovalent cations in forsterite $Mg_2SiO_4$ and diopside $CaMgSi_2O_6$, where the O—O interactions for these alkali silicate potentials are kept the same as the Sanders *et al.* parameters [10] and the two sets of potentials are hence fully compatible. These alkali-oxygen parameters were derived by fitting to the experimental lattice structures and elastic data of the relevant binary oxides and the applicability of these alkali potential parameters in silicate materials was shown in Purton *et al.*'s work [14] as well as, for example, in studies by Van Weston *et al.* [15]. The complete potential model used in this work is provided in table 1.

### 2.2 Combinatorial analysis and statistics of cation distributions

We have chosen three experimental disilicates as starting structures for the simulations of Li–K solid solutions, namely two single alkali disilicate materials ($Li_2Si_2O_5$ and $K_2Si_2O_5$) and one mixed alkali disilicate containing equal amounts of lithium and potassium ($KLiSi_2O_5$). The approach used to study the cation distributions for each composition was to consider all the different substitutions of Li and K in the cationic sites of a variety of supercells of the original unit cell, gradually replacing the existing

Table 1. Potential parameters used in this work.

| *Charges (e)* *Ion* | *Core* | *Shell* | *Core-shell interaction* ($eV\AA^{-2}$) |
|---|---|---|---|
| Silicon | +4.00000 | | |
| Oxygen | +0.84819 | −2.84819 | 74.92038 |
| Lithium | +1.00000 | | |
| Potassium | +1.00000 | | |
| | Buckingham Potential | | |
| Inter-molecular | A (eV) | ρ (Å) | C ($eV\AA^6$) |
| $Si^{4+}$—$O^{2-}$ * | 1283.91 | 0.32052 | 10.66158 |
| $O^{2-}$—$O^{2-}$ * | 22764.0 | 0.14900 | 27.88 |
| $Li^{+}$—$O^{2-}$ † | 262.54 | 0.3476 | 0.0 |
| $K^{+}$—$O^{2-}$ † | 680.4384 | 0.3798 | 0.0 |
| | Three-body Potential | | |
| | K ($eV\,rad^{-2}$) | | $\Theta_0$ |
| $O_{shell}{}^{2-}$—Si—$O_{shell}{}^{2-}$ * | 2.09724 | | 109.470000 |

* Reference [10]. † Reference [14].

lithium with potassium or vice versa, followed by energy minimisation of the resulting configurations. If $M$ is the total number of available cation sites in a particular supercell and $n$ is the number of potassium ions in each composition, then there will be $N$ ways of distributing these $n$ potassium ions over the $M$ cationic sites, as shown in equation (1):

$$N = \frac{M!}{n!(M-n)!} \tag{1}$$

However, if we consider the symmetry of the disilicate structures, the number of non-identical configurations for each composition can be reduced from the total number of configurations obtained from equation (1). The symmetry equivalence between configurations was determined by obtaining first the symmetry operators of the generic (non-substituted) supercell; then two given distributions of substitutions (Li,K) are equivalent if any of the symmetry operations converts one configuration into the other. Having developed a computer program based on this procedure, it was possible to identify and generate all the different cationic configurations for each supercell [16]. For $Li_2Si_2O_5$ and $KLiSi_2O_5$ the simulation supercells contain eight cation sites each and a series of calculations has been performed, where the ratio of potassium to total cations equals 0, 0.125, 0.25 0.5, 0.625, 0.75 and 1.0. For $K_2Si_2O_5$ a primitive cell with twelve cation sites was generated and structures with K ratios of 0.0, 0.083, 0.167, 0.25, 0.33, 0.417, 0.5, 0.583, 0.67, 0.75, 0.833, 0.917 and 1.0 have been studied. For each composition all non-equivalent cation distributions across the cation sites are considered and the number of non-identical configurations for each composition, which have been calculated in this work, are listed in table 2. Despite the reduction in the number of configurations that we need to consider, due to the use of symmetry arguments to obtain non-equivalent cation distributions, this comprehensive study still necessitates very large numbers of independent calculations.

### *2.3 Condor pool technology*

As each separate calculation is not particularly compute intensive, we have run the simulations on a Condor pool of modest PC's, which was recently developed within University College London to harvest otherwise idle computing resources to utilise for research purposes. Presently, the pool comprises 900 + nodes, mainly made up of Pentium-3 teaching PC clusters, running the Windows operating system. All machines are centrally managed, network-booted with one of 8 Windows terminal server (WTS) thin-client images, facilitating expedient distributed software deployment and re-engineering. Additionally, the current thin client architecture requires very few local CPU cycles. Crucially, only 5% of the available CPU cycles have historically been used. Harnessing the remaining 95% of CPU cycles across the cluster network had the potential to create, cheaply and efficiently, an ideal resource for scientists to compute the types of problems where the actual amount of power required for an individual job is relatively low—comparable to an average desktop PC—and parallelisation is not required, but where often many (thousands or more) runs of the same program, each with a different set of input parameters, are required.

In addition, the UCL Condor pool is part of wider grid-based resources with a common infrastructure for running codes on similar sets of data, requiring interchange of data and hence interoperability between codes. Full technical details of the Condor pool and its place in this computational and data grid system is described elsewhere in this issue.

## 3. Results and discussion

For each of the three disilicate materials, the stabilities of the mixed-cation compositions were assessed by calculating the excess heat of solid solution of the materials, according to equation (2):

$$\Delta E_x(\mathrm{Li,K}) = E(\mathrm{Li}_{1-x}\mathrm{K}_x) - \{[1-x]E(\mathrm{Li}) + xE(\mathrm{K})\} \tag{2}$$

where ($\Delta E_x$(Li,K) is the excess heat of mixing of the lithium and potassium end-members, $E(\mathrm{Li}_{1-x}\mathrm{K}_x)$ is the energy of the mixed solid, and $[1-x]E$(Li) and $xE$(K) are the energies of identical fractions of the pure lithium and potassium end-members to the mixed solid under consideration. The excess heat of mixing hence demonstrates the relative stability of the mixed phase with

Table 2. Number of non-identical configurations for each composition in three different Li–K-silicates.

| | | | | | | | | | | | | | |
|---|---|---|---|---|---|---|---|---|---|---|---|---|---|
| | | | | | | *$Li_2Si_2O_5$ Structure* | | | | | | | |
| K content/% | 0 | 0.125 | 0.250 | 0.375 | 0.500 | 0.625 | 0.750 | 0.875 | 1 | | | | |
| Number of configurations | 1 | 1 | 7 | 7 | 14 | 7 | 7 | 1 | 1 | | | | |
| | | | | | | *$KLiSi_2O_5$ Structure* | | | | | | | |
| K content/% | 0 | 0.125 | 0.250 | 0.375 | 0.500 | 0.625 | 0.750 | 0.875 | 1 | | | | |
| Number of configurations | 1 | 2 | 10 | 14 | 22 | 14 | 10 | 2 | 1 | | | | |
| | | | | | | *$K_2Si_2O_5$ Structure* | | | | | | | |
| K content/% | 0 | 0.083 | 0.167 | 0.250 | 0.333 | 0.417 | 0.500 | 0.583 | 0.667 | 0.75 | 0.833 | 0.917 | 1 |
| Number of configuration | 1 | 6 | 36 | 110 | 255 | 396 | 472 | 396 | 255 | 110 | 36 | 6 | 1 |

respect to the same quantities of the pure materials. An early study of solid solutions of simple oxides by Catlow and co-workers, using interatomic potential methods with full lattice relaxation, showed good agreement between experimental and theoretical heats of mixing [17], while later work comparing these computational methods with *ab initio* Hartree Fock calculations [18] and DFT calculations of more complex oxides [19] demonstrated again that full lattice relaxation is needed to reproduce experimental enthalpies of mixing, which is therefore the practice we have followed in this work. All simulations are hence conducted as constant pressure calculations, where not only the atomic coordinates but also the cell shape and volume are allowed to vary during the geometry optimisation.

### 3.1 $Li_2Si_2O_5$ Structure

The first of the three disilicates used for our solid solution calculations is the lithium phyllosilicate $Li_2Si_2O_5$ structure determined by de Jong *et al.* [20], which has the space group CCC2 and a unit cell of $a = 5.81$ Å, $b = 14.58$ Å, $c = 4.77$ Å and $\alpha = \beta = \gamma = 90°$. On geometry optimisation, the unit cell parameters relax to $a = 5.97$ Å, $b = 14.75$ Å, $c = 4.94$ Å and $\alpha = \beta = \gamma = 90°$ and the optimised structure is shown in figure 1(a), (b) (the alkali ions in figure 1 have been omitted for clarity). Although the individual lattice vectors have lengthened somewhat, the experimental *c*/*a* ratio of 0.82 has been reproduced by the simulation ($c/a = 0.83$) and the experimental structure has been retained. The cell contains eight alkali ions, eight silicon atoms and twenty oxygen atoms. The silica sheet in this lithium phyllosilicate is composed of a framework of six-membered rings of silica tetrahedra in the $a$–$c$ plane, featuring a symmetric "chair" structure in the $a$–$b$ plane (figure 1(a), (b)). The lithium ions, which are located between the silica layers, link the non-bridging oxygen atoms to support the layered structure. The ring structures are thus two-dimensional and do not form continuous channels throughout the structure.

One by one, the lithium ions in the initial structure are replaced by potassium ions. For each composition the

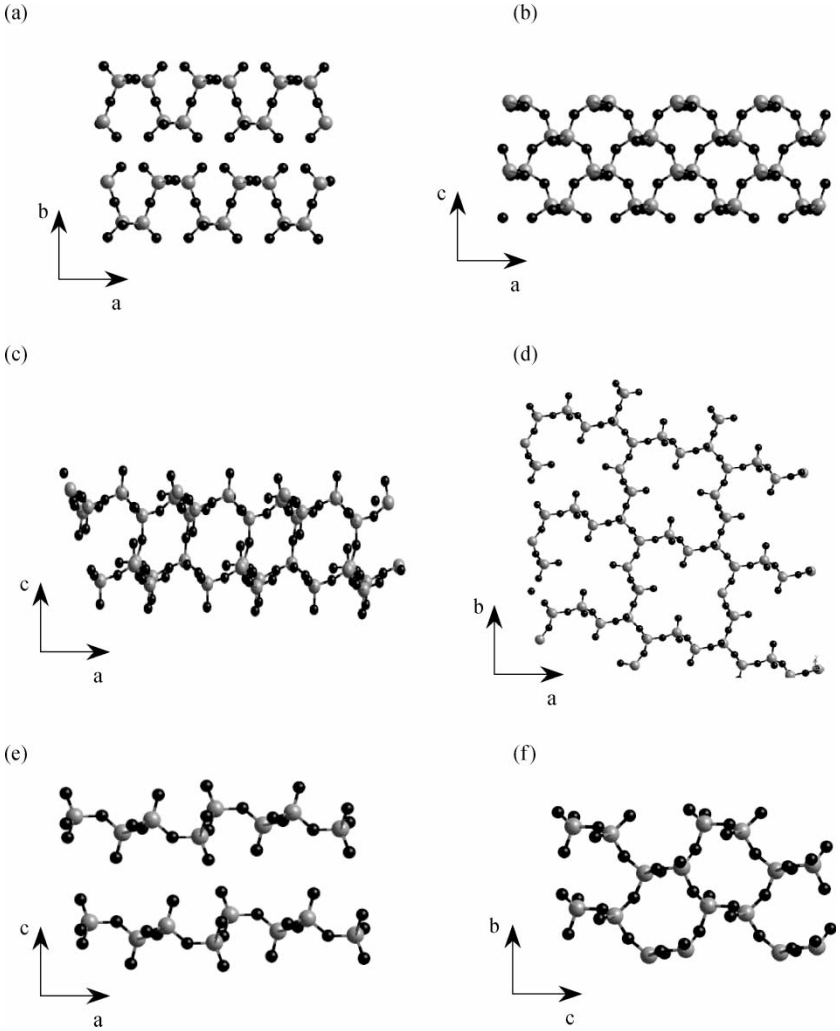


Figure 1. Geometry optimized structures of the three different disilicate materials: $Li_2Si_2O_5$ (a) view of $a$–$b$ plane and (b) view of $a$–$c$ plane; $K_2Si_2O_5$ (c) view of the $a$–$c$ plane and (d) view of the $a$–$b$ plane; and $LiKSi_2O_5$ (e) view of the $a$–$c$ plane and (f) view of the $b$–$c$ plane (Si = grey, O = black, alkali ions have been omitted for clarity).

lattice energies of all non-identical configurations are calculated and the energy distribution for each composition over the whole concentration range is displayed in figure 2a, where the configuration with the lowest energy for each composition is selected for analysis and discussion. When we compare the highest energy structures with the lowest energy ones for each composition, we find that in all high-energy configurations either the silica layers have collapsed or at least one of the silica sheets is destroyed, whereas the original layered structure has been retained in the low-energy structures.

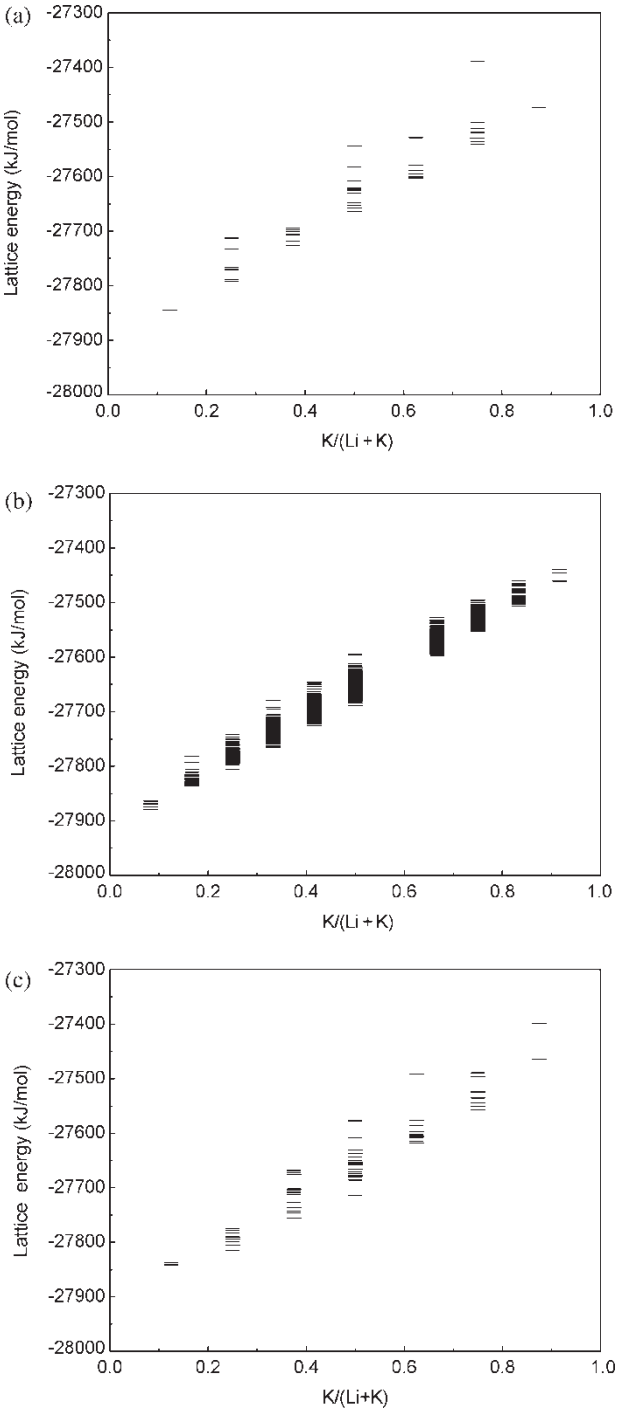


Figure 2. Spread of lattice energies over the non-equivalent configurations for the different Li–K compositions, for (a) structures based on $Li_2Si_2O_5$, (b) structures based on $K_2Si_2O_5$ and (c) structures based on $LiKSi_2O_5$.

The calculated excess heats of solid solution from equation (2) are plotted against the concentration of potassium in figure 3a. It is clear that the replacement of the first lithium ion by a potassium atom ($x = 0.125$) is energetically unfavourable, which may be due to the size difference between the lithium and potassium ions. The potassium ion, with an ionic radius of $r = 1.33$ Å, is twice as big as the lithium ion ($r = 0.68$ Å) [21] and when the bigger potassium is introduced at the lithium lattice site, there is not enough room to accommodate the potassium ion without significant distortion of the lattice, which is energetically unfavourable. The effect on the structure of incorporating the first potassium is to increase the lattice vector $b$ by about 9%, with a concurrent distortion of the angles from $\alpha = \beta = \gamma = 90°$ to $\alpha = 93.5°$, $\beta = 89.2°$ and $\gamma = 95.68°$.

However, further incorporation of potassium in the lithium lattice sites is either energetically neutral ($x = 0.25$) or even energetically favourable at higher K concentrations, indicating that once the lattice has accommodated the first potassium, incorporation of further potassium is much easier. When studying the change in structure of the initial $Li_2Si_2O_5$ material with increasing potassium content, we see that the silicate sheet remains built up of the six-membered rings of silica tetrahedra in the $a$–$c$ plane, which was seen in the pure lithium phyllosilicate structure. However, with the increasing amount of potassium in the structure, the symmetric chair conformation shown in figure 1a has been destroyed and the symmetric structure is only recovered when all lithium ions have been replaced by potassium ions, i.e. for a pure $K_2Si_2O_5$ structure.

### 3.2 $K_2Si_2O_5$ structure

Unlike $Li_2Si_2O_5$, the $K_2Si_2O_5$ material is not a phyllosilicate but has a three-dimensional defective cristobalite structure with space group CC. The experimental data from the work of De Jong *et al.* [20] are used to construct our second disilicate structure, this time studying the effect of lithium incorporation in an experimental potassium material. The unit cell is $a = 9.91$ Å, $b = 9.91$ Å, $c = 9.92$ Å, $c/a = 1$ and $\alpha = 68.8°$, $\beta = 111.1°$ and $\gamma = 110.9°$, which is geometry optimised to give $a = 10.36$ Å, $b = 10.36$ Å, $c = 10.36$ Å, $c/a = 1$ and $\alpha = 70.2°$, $\beta = 109.8°$ and $\gamma = 109.8°$, with twelve alkali ion sites in the structure. The structure, shown in figure 1(c,d), is built up of 14-membered-rings in the $a$–$b$ plane (figure1(d)) with a chair conformation of silica sheets in the $a$–$c$ and $b$–$c$ planes. In contrast to the lithium disilicate structure, the layers in this potassium disilicate are connected by six-membered rings rather than the alkali ions, leading to a three-dimensional framework but still with a layered character.

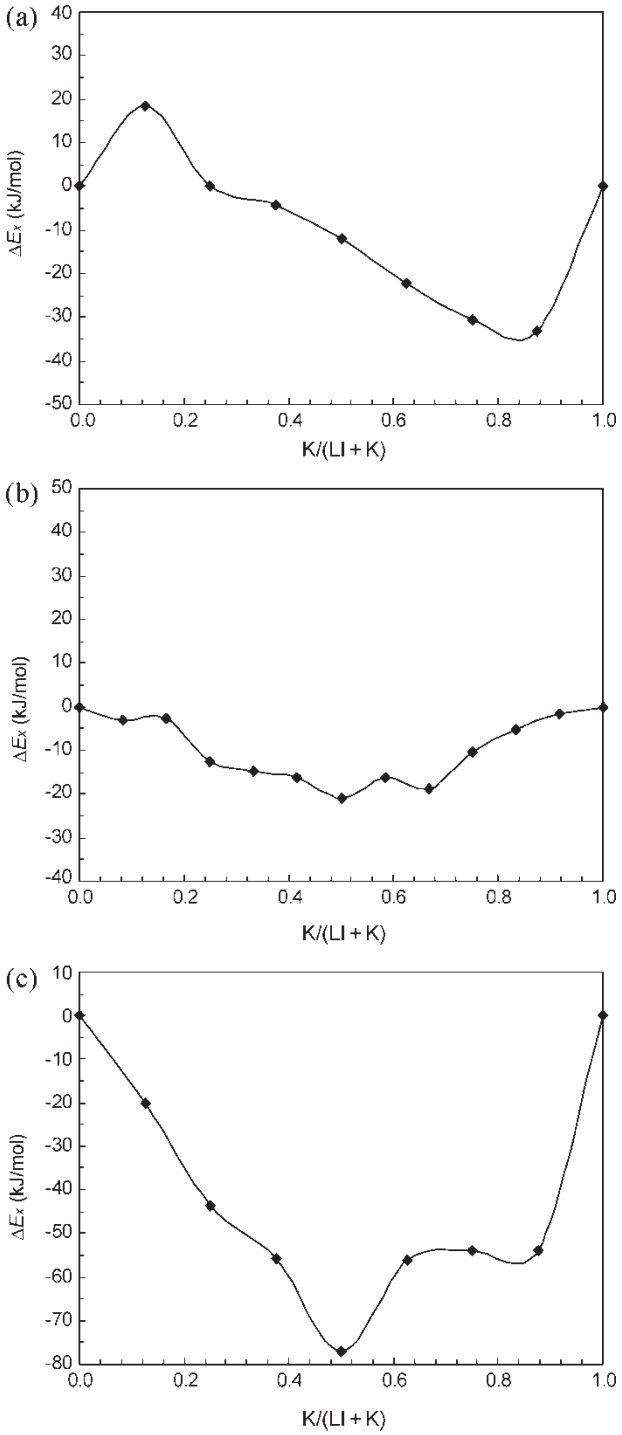


Figure 3. Plots of the variation of excess heat of solid solution with potassium content, for (a) structures based on $Li_2Si_2O_5$, (b) structures based on $K_2Si_2O_5$ and (c) structures based on $LiKSi_2O_5$.

In this material, the number of non-identical configurations for each composition varies from 1–472 and overall we needed to calculate 2080 non-identical configurations for the complete range of Li–K solid solutions. The energy distribution of the different non-equivalent configurations versus potassium content is shown in figure 2(b). The 14-membered ring structures for all compositional configurations remain virtually identical and the incorporation of the smaller lithium ions into the bigger potassium lattice sites does not significantly disturb the silicate framework. The excess heats of solid solution for this structure are plotted in figure 3(b) from which we see that the Li–K solid solutions are energetically stable with respect to the two end-members for all compositions, in contrast with the $Li_2Si_2O_5$-based structures shown in figure 3(a). The lack of distortion of the original structure upon incorporation of lithium ions plus the negative Li–K solid solution energies of this potassium-based structure is in agreement with McLean, who proposed that the incorporation of impurity cations is governed by the reduction in elastic strain [22]. Hence, incorporation of the smaller lithium ion at potassium sites should not lead to an increased elastic strain in the potassium disilicate lattice and hence the solid solution would be stable.

From figure 3(b) we note that the composition with equal amounts of lithium and potassium is marginally more stable than the other compositions, which is due to ordering of the alkali ions within the lattice. The $a-c$ and $b-c$ planes, shown in figure 1(c) contain one-dimensional channels into the $b$ and $a$ directions, respectively. Initially these channels are filled by potassium ions, but when these are substituted by lithium ions, these lithium ions fill the potassium sites in an ordered manner, for the 50/50 mixture leading to an alternation of channels filled with either lithium or potassium ions only and channels filled with both alkali ions in a ratio of Li:K $= 1$, with the potassium located centrally within the channels and the lithium ions at the edges. For lower lithium loadings, these alternating channels are only partially formed and for the 25% solid solutions only in one direction (along the $a$ or $b$ vector). However, full ordering in both directions is obtained in the 50/50 mixture, leading to the enhanced stability for this composition.

### 3.3 $KLiSi_2O_5$ structure

We finally examined a second phyllosilicate structure which in nature already contains both cations in a fully ordered fashion. The $KLiSi_2O_5$ structure used for this final set of simulations was determined by De Jong and co-workers [23], with a monoclinic structure with space group P 21 and a unit cell of $a = 5.98$ Å, $b = 4.80$ Å and $c = 8.16$ Å, $c/a = 1.36$ and $\alpha = \gamma = 90°$ and $\beta = 93.5°$, which is geometry optimised to give $a = 6.45$ Å, $b = 4.99$ Å and $c = 8.47$, $c/a = 1.31$ Å and $\alpha = \gamma = 90°$ and $\beta = 94.8°$. We constructed a supercell of two basic unit cells, containing a total of 36 atoms and eight alkali ion sites. Again, we investigated all possible configurations of a range of Li–K solid solutions of this mixed structure, which is shown in its pure form in figure 1(e),(f). The structure contains silica sheets in a chair conformation similar to that observed in the pure $Li_2Si_2O_5$ material and the silica layers are again linked by alkali ions. However, unlike the chair conformations in the $Li_2Si_2O_5$, the 'chairs' here are no longer symmetric. In addition, the six-membered rings of silica tetrahedra now form continuous channels throughout the structure, which feature is not observed in the other two structures.

The energy distributions of the non-equivalent configurations for each cation ratio are shown in figure 2(c). In general, the energy gap for each composition is smaller in the range of $K/(K + Li) < 0.5$ indicating that the introduction of substitutional lithium ions up to the 50/50 structure has little effect on the lattice, similar to the situation where the smaller lithium ion was incorporated into the $K_2Si_2O_5$ structure. However, when potassium atoms come to dominate the structure (i.e. $K/(K + Li) > 0.5$), the energy gap between low- and high-energy structures becomes wider, comparable to the introduction of potassium into the $Li_2Si_2O_5$ structure. Again, these effects are all in agreement with the theory by McLean that the incorporation of impurity ions is governed by the elastic strain on the lattice [22].

The excess heats of solid solution are plotted against each composition in figure 3(c). Once again, the solid solutions are stable with respect to the pure end-members across the whole range, but in this case there is a very marked minimum energy structure at $K/(Li + K) = 0.5$. This particularly stable position at a 50/50 composition of lithium and potassium is not surprising as the experimental starting structure for this range of solid solutions already contained an equal number of Li and K ions. Not surprisingly, the calculated minimum energy structure for the composition of $K/(K + Li) = 0.5$ is the same as the experimental structure [23].

The major features of the experimental starting structure, i.e. the 'chain' of silica tetrahedra in asymmetric chair conformations, the alkali ions sandwiched between the silica layers, and the six-membered rings in the $b-c$ plane forming continuous channels throughout the lattice, appear in all lowest-energy configurations for a wide range of potassium content. In the mixture with equal amounts of potassium and lithium, i.e. four potassium ions and four lithium ions, shown in figure 4 (b), the four potassium ions reside approximately in the centre of the six-membered rings whereas the four lithium ions are situated at the edge of the rings, shown in figure 4(b) where two lithium ions cannot be seen as these are located on the other side. When the potassium content in the mixture becomes more than 50%, (shown for example in figure 4(c)), the extra potassium ions also become located at the edge of the rings, in the lithium sites. However, when the potassium concentration is lower than 50% (see figure 4 (a)), some lithium ions enter the unoccupied channel positions, whereas the rest of the lithium remains at the edge of the channel. A loss or surplus of potassium thus does not lead to the occupation of interstitial positions and consequent creation of vacancies in the original lattice. However, our calculations show that mixed Li–K structures where the larger potassium ion resides in the centre of the channel are in all cases thermodynamically more stable than structures where the smaller lithium ions are located in the channel positions, in agreement with the original experimental structure [23].

### *3.4 Structure comparison*

Although all three original materials contain rings of silica tetrahedra, there are distinct differences between the three structures. In the case of the phyllosilicates, $KLiSi_2O_5$ and $Li_2Si_2O_5$, six-membered rings in a chair conformation are formed, although the chairs are asymmetric in $KLiSi_2O_5$ but symmetric in $Li_2Si_2O_5$. However, the sizes of the six-membered rings in $Li_2Si_2O_5$ and $KLiSi_2O_5$ are very similar with diameters of 5.9 and 6.2 Å respectively. The ring structure in $K_2Si_2O_5$, on the other hand, made up of 14 silica tetrahedra, is not as symmetric and much larger, with a diameter of about 13.9 Å. Strictly speaking this structure is not layered in the same sense as the phyllosilicates, where the alkali ions link the sheets of $SiO_4$ tetrahedra, as the layers in the $K_2Si_2O_5$ material are connected by Si—O—Si bridges, leading to an open three-dimensional framework.

As a result of these structural differences, the response of the lattice to the variation in Li–K composition is subtly different for the three materials. The structure of the lithium compound is destroyed completely by the incorporation of potassium, although the six-membered rings are retained, whereas the potassium material is hardly distorted by the substitutional incorporation of lithium and retains its original structure throughout the compositional series. The Li or K endmembers obtained from the mixed $KLiSi_2O_5$ compound show an interesting structural variation of the silica layers, depending on the type of alkali ion incorporated in the lattice. Liebau suggested that flat sheets of $SiO_4$ tetrahedra, which were charge-compensated by singly charged cations, were only possible if the cations between the sheets were of sufficient size to to fill the available space between the tetrahedra [21]. Only the francium ion has the required size to fill this space and Liebau proposed that charge compensation by all other, smaller alkali ions would then lead to buckling of the silica sheets, where the extent of buckling was dependent on the size of the cation, with the

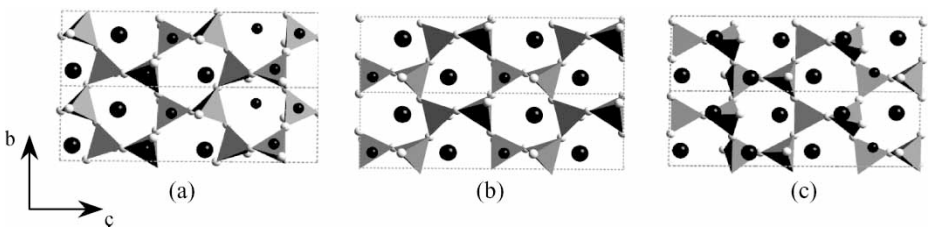


Figure 4. View of the $b-c$ plane of different compositions of mixed potassium lithium phyllosilicate (a) K:Li = 3:5. (b) K:Li = 4:4 (c) K:Li = 7:1 (Li = black (small), K = black (big), Si = grey and O = white).

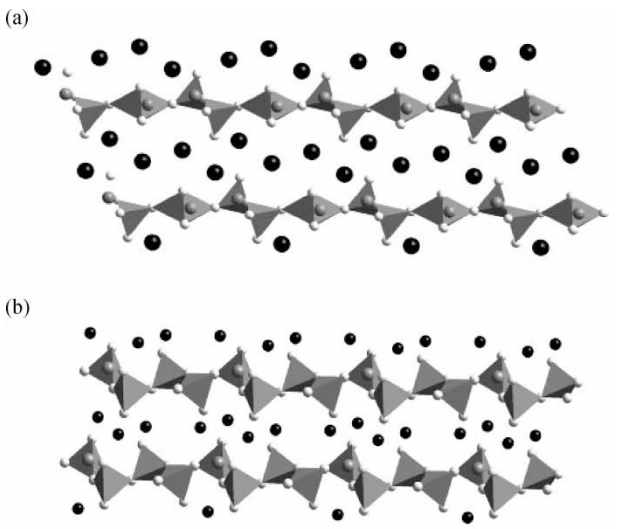


Figure 5. The mixed $LiKSi_2O_5$ structure, (a) with all Li ions substituted by K ions and (b) with all K ions substituted by Li ions.

smallest Li ion leading to the most extensive buckling. His theory is borne out by our simulations of the $KLiSi_2O_5$ structure, where the silica sheets respond to an increase of lithium or potassium ions by an increase or decrease, respectively, in buckling of the silica sheet. Figure 5 shows the mixed $KLiSi_2O_5$ structure, either fully loaded with potassium (figure 5(a)) or fully loaded with lithium (figure 5(b)), clearly showing the flatter $SiO_4$ sheet in the potassium structure compared to the lithium structure, which is now similar to the original $Li_2Si_2O_5$ material as far as the extent of buckling of the sheets is concerned.

In figure 6, we have compared the calculated lattice energies of all three layered silicate materials over a wide range of Li–K compositions. It is clear that for the range of $K/(Li + K) = 0.2–0.8$, the structures obtained from the mixed $KLiSi_2O_5$ material are more stable than those obtained from the other two structures. However, at lower potassium contents in the mixture (e.g $K/(Li + K) < 10\%$) we see that the $Li_2Si_2O_5$-type structures are preferred,

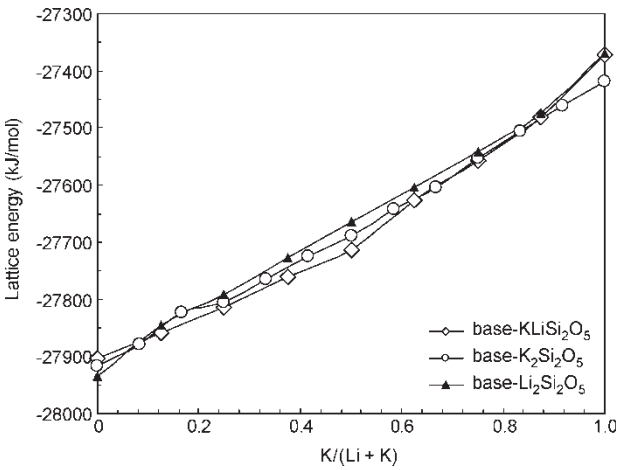


Figure 6. Comparison of calculated lattice energies for each composition of the three disilicate materials.

whereas the $K_2Si_2O_5$-type structure is energetically the most favourable structure for mixtures dominated by potassium ($K/(Li + K)$ over 85%). These findings are perhaps not surprising as they confirm the natural disilicate materials as the most stable structures for particular Li–K compositions, but they do show that the preference for these structures in the natural environment is borne out by their relative thermodynamic stabilities and is not based on kinetic factors.

## 4. Conclusions

Classical energy minimization techniques have been used to investigate the effects of a range of Li–K distributions on the structures and stabilities of a series of layered K–Li disilicate materials. Many thousands of independent calculations were carried out to calculate all possible configurations of the Li–K solid solutions over a wide range of compositions.

Our results show that all structures are amenable to the full range of solid solutions, they are derived from an experimental lithium compound, a pure potassium material or the mixed Li–K disilicate. However, the relative stabilities of the mixed configurations reflect the structures of the natural materials, where the preference for a particular starting structure ranges from $Li_2Si_2O_5$ for a potassium content of less than 10% through $KLiSi_2O_5$ for a potassium content between 20–80% and $K_2Si_2O_5$ at a potassium content of over 85%.

Our simulations indicate that with increasing potassium content the silica layers prefer different configurations, even though phase transitions between the three structures cannot be deduced from these particular calculations. At a low concentration of potassium, the silica tetrahedra form six-membered rings in highly buckled sheets, in agreement with Liebau's theory. In the middle range of potassium content, the symmetry of the "chair" conformation has been destroyed and the six-membered rings now form continuous channels through the structure, whereas at high potassium concentrations, the structure of individual silica sheets with intercalated cations has disappeared and very large silica rings are formed, which are connected by Si—O—Si bridges in an open three-dimensional framework.

This study was enabled by the use of the UCL Condor pool of PC's, which has successfully harnessed unused computational teaching resources for research. Future work will include additional solid solution calculations of the complete range of alkali and alkali earth ions into these materials, to further investigate Liebau's predictions of the effects of cation charges and sizes on structural variations in layered silicates.

## Acknowledgements

We acknowledge NERC, grant no. NER/T/S/2001/00855, for financial support under the UK e-Science initiative.

NHdL thanks EPSRC for an Advanced Research Fellowship and Dr J.C. Phillips for useful discussions.

## References


[1] D.E. Day. Mixed alkali glasses – their properties and uses. *J. Non-Cryst. Solid*, **21**, 343 (1976).

[2] M.D. Ingram. Ion conductivity in glass. *Phys. Chem. Glasses*, **28**, 215 (1987).

[3] J.O. Isard. The mixed alkali effect in glass. *J. Non-Cryst. Solid*, **1**, 235 (1969).

[4] J. Habasaki, I. Okada, Y. Hiwatari. MD study of the mixed alkali effect in a lithium–potassium metasilicate glass. *J. Non-Cryst. Solid*, **1**, 235 (1995).

[5] H. Matsumoto, Y. Shigesato, I. Yasui. Molecular dynamics study on structure and energetic property of single and mixed alkali glasses. *Phys. Chem. Glasses*, **37**, 212 (1996).

[6] D. Thain, T. Tannenbaum, M. Livny. Condor and the Grid. In *Grid Computing: Making the Global Infrastructure a Reality*, F. Berman, A.J.G. Hey, G. Fox (Eds.), John Wiley, Chichester, UK (2003).

[7] M. Born, K. Huang. *Dynamical Theory of Crystal Lattices*, Oxford University Press, Oxford (1954).

[8] B.G. Dick, A.W. Overhauser. Theory of the dielectric constants of alkali halide crystals. *Phys. Rev.*, **112**, 90 (1958).

[9] G.W. Watson, E.T. Kelsey, N.H. de Leeuw, D.J. Harris, S.C. Parker. Atomistic simulation of dislocations, surfaces and interfaces in MgO. *J. Chem. Soc. Farad. Trans.*, **92**, 433 (1996).

[10] M.J. Sanders, M. Leslie, C.R.A. Catlow. Interatomic potentials for $SiO_2$. *Chem. Commun.*, **19**, 1271 (1984).

[11] N.H. de Leeuw, F.M. Higgins, S.C. Parker. Modelling the surface structure and stability of α-quartz. *J. Phys. Chem. B*, **103**, 1270 (1999).

[12] F.M. Higgins, N.H. de Leeuw, S.C. Parker. Modelling the effect of water on cation exchange in zeolite A. *J. Mat. Chem.*, **12**, 124 (2002).

[13] N.H. de Leeuw, S.C. Parker, C.R.A. Catlow, G.D. Price. Modelling the effect of water on the surface structure and stability of forsterite. *Phys. Chem. Miner.*, **27**, 332 (2000).

[14] J.A. Purton, N.L. Allan, J.D. Blundy. Calculated solution energies of heterovalent cations in forsterite and diopside: Implications for trace element partitioning. *Geochim. Cosmochim. Acta*, **61**, 3927 (1997).

[15] W. van Westrenen, N.L. Allan, J.D. Blundy, J.A. Purton, B.J. Wood. Atomistic simulation of trace element incorporation into garnets-comparison with experimental garnet-melt partitioning data. *Geochim. Cosmochim. Acta*, **64**, 1629 (2000).

[16] R. Grau-Crespo, N.H. de Leeuw, C.R.A. Catlow. Distribution of cations in $FeSbO_4$: A computer modeling study. *Chem. Mater.*, **16**, 1954 (2004).

[17] C.R.A. Catlow, B.E.F. Fender, P.J. Hampson. Thermodynamics of MnO + CoO and MnO + NiO solid solutions. *J. Chem. Soc. Farad. Trans. 2*, **73**, 911 (1977).

[18] M. Königstein, F. Corà, C.R.A. Catlow. An *ab initio* Hartree-Fock study of the energies of mixing of MnO–NiO, MgO–MnO and CaO–MnO solid solutions. *Solid State Chem*, **137**, 261 (1998).

[19] N.H. de Leeuw. Density functional theory calculations of solid solutions of fluor-and chlorapatites. *Chem. Mater.*, **14**, 435 (2002).

[20] B.H.W.S. De Jong, H.T.J. Supèr, A.L. Spek, N. Veldman, G. Nachtegaal, J.C. Fischer. Mixed alkali systems structure and $^{29}$Si MASNMR of $Li_2Si_2O_5$ and $K_2Si_2O_5$. *Acta Cryst. B*, **54**, 568 (1998).

[21] F. Liebau. Ein Betrag zur Kristallchemie der Schichtsilikate. *Acta Cryst. B*, **24**, 690 (1968).

[22] D. McLean. *Grain Boundaries in Metals*, Clarendon Press, Oxford (1957).

[23] B.H.W.S. De Jong, H.T.J. Supèr, A.L. Spek, N. Veldman, W. Van Wezel, V. Van der Mee. Structure of $KLiSi_2O_5$ and the hygroscopicity of glassy mixed alkali disilicates. *Acta Cryst. B*, **52**, 770 (1996).